

Comparison study of the MRI shoulder PROPELLER technique with differential image quality by variation of shoulder coils

Mohamad Khairi Mahmood@Ab Hamid, MSc^{1,2}, Faikah Zakaria@Mahmod, MSc¹, Rafidah Supar, MSc¹, Zanariah Mohd, PhD¹

¹Centre for Medical Imaging Studies, Faculty of Health Sciences, Universiti Teknologi MARA (UiTM) Selangor, Puncak Alam Campus, Selangor, Malaysia, ²Radiology Department, Hospital Pengajar UPM, University Putra Malaysia, Serdang, Selangor, Malaysia

ABSTRACT

Introduction: Motion and pulsation artifacts are the most prominent types of artifacts in Magnetic Resonance Imaging (MRI) of the shoulder. Therefore, this study examined the Periodically Rotating Overlapping Parallel Lines with Enhanced Reconstruction (PROPELLER) technique with small flex coil (SFC) and dedicated shoulder coil (DSC) for the reduction of motion and pulsation artifacts. The signal-to-noise ratio (SNR) and contrast-to-noise ratio (CNR) of the standard proton density fat saturation (PDFS) pulse sequence and the PROPELLER proton density fat saturation (PROPELLER PDFS) pulse sequence were also evaluated.

Materials and Methods: Eighteen (18) participants who met the inclusion and exclusion criteria were scanned using a standard non-contrast MRI shoulder protocol including the PDFS pulse sequence and the PROPELLER PDFS pulse sequence using a small flex coil and a dedicated shoulder coil. Two experienced musculoskeletal (MSK) radiologists evaluated and graded the presence of artifacts on the MR images and the SNR and CNR were measured quantitatively.

Results: The non-parametric Wilcoxon Signed Rank test revealed a significant reduction in motion and pulsation artifacts between the PROPELLER PDFS pulse sequence and the standard PDFS pulse sequence. In addition, the nonparametric Mann-Whitney U test revealed that the mean rank of SNR for the standard sequence was statistically significant when compared to the PROPELLER sequence for both coil types. The CNR of the PROPELLER sequence was statistically significant between fat-fluid, bone-fluid, bone-tendon, bone-muscle, and muscle-fluid when using SFC and DSC.

Conclusion: This study proved that the PROPELLER-PDFS pulse sequence effectively eliminates motion and pulsation artifacts, regardless of the coils utilised. The PROPELLER-PDFS pulse sequence can therefore be implemented into the standard MRI shoulder procedure.

KEYWORDS:

MRI shoulder, PROPELLER, PDFS, coil, artifact

INTRODUCTION

Imaging the musculoskeletal (MSK) system is a valuable diagnostic approach for determining the causes of shoulder disease and formulating the best treatment strategy. MRI with high resolution permits the identification of the tendon, muscle, and ligament in the shoulder. King, Healy and Baird,¹ highlighted that MRI is necessary for evaluating the symptom of tendinopathy since it can evaluate the rotator cuff associated with the bone structure, muscles, tendons, and adjacent soft tissues.

The utilisation of MRI for diagnosing MSK and shoulder diseases has both advantages and disadvantages. The MRI technique has significantly contributed to the enhancement of clinical disease diagnosis, treatment planning, and response evaluation. Furthermore, there is an increasing trend of employing MRI in research investigations focused on musculoskeletal conditions, including shoulder. MRI is an imaging modality that provides additional information on cartilage, inflammation, and injury or degeneration of surrounding soft tissue structures² and can identify and monitor abnormalities in their initial phases.³

Besides providing excellent soft tissue contrast and high-resolution images, MRI of the shoulder is susceptible to image degradation from various patient motion sources, including respiration and uncooperative patients as well as pulsatile flow, which can significantly impact the image quality and diagnostic value of MRI.⁴ According to Goh and Peh,⁵ the random motion artifact results from uncooperative patients or pain or discomfort severity. This artifact remains a significant issue in clinical and research MRI applications. The primary appearances of motion artifact are ghosting and blurring, which occur when the patient moves during data acquisition in the k-space using the Cartesian method.⁶ Numerous strategies were proposed to rectify the motion artifact, which can be divided into three categories: 1)prevention of motion by restricting the patient's movement during the scanning process, 2)motion correction techniques, and 3)artifact reduction.⁷ The use of pads and cushions to prevent motion artefacts is ineffective and often inconvenient for long scanning durations.⁸ Motion correction techniques have tremendous potential, but they have not been thoroughly validated and require additional hardware or

This article was accepted: 29 October 2023

Corresponding Author: Faikah Zakaria

Email: faikah@uitm.edu.my

pulse sequence modifications.⁹ In numerous MRI studies, artifact reduction techniques such as ordered phase encoding¹⁰ and Periodically Rotating Overlapping Parallel Lines with Enhanced Reconstruction (PROPELLER), have been demonstrated to effectively reduce motion.¹¹ By using Periodically Rotating Overlapping Parallel Lines with Enhanced Reconstruction (PROPELLER), image artifacts such as motion artifacts and magnetic susceptibility artifacts can be reduced¹² and the limitations of the MRI can be addressed.^{13,14}

The PROPELLER technique was developed to reduce motion artifacts by employing radial k-space coverage. It has been implemented to decrease pulsation and motion artefacts.^{11,15-16} Unfortunately, the PROPELLER method produces streak artifacts in MRI images. The MRI images develop streak artifacts because of the under-sampling that occurs during the gridding phase, which transforms the location of the incoming data through complementing processing from an oblique trajectory to an accurate grid in k-space.¹⁶

Shoulder MRI typically uses a dedicated shoulder RF coil or a small flex RF coil. The dedicated shoulder RF coil operates as a transmitter and receiver (transceiver) coil; meanwhile, the small flex coil operates solely as a receiver coil. The type, size, and position of the RF coil in relation to the patient's body can impact the overall MR image quality. According to Mulyati et al.,¹⁷ the signal-to-noise (SNR) and contrast-to-noise (CNR) ratios of the dedicated shoulder coil are greater than those of the small flex coil. With the invention of the first solenoids, several factors, including coil homogeneity, self-resonance, efficiency, quadrature detection, transmission line effects, and quality factor, have significantly influenced the design of RF coils.¹⁸ Thus, this research aimed to examine the MRI shoulder PROPELLER technique with differential image quality based on shoulder coil variation. In addition, this research examined the reduction of motion and pulsation artifacts and compared the SNR and CNR between standard coronal oblique proton density fat saturation (PDFS) and coronal oblique PROPELLER proton density fat saturation (PROPELLER PDFS) pulse sequences.

MATERIALS AND METHODS

Participants

The study included 18 participants who met the inclusion and exclusion criteria (Table I) and was conducted from November 2022 to January 2023. All participants were given a subject information sheet and consent form before scanning. Participants who agreed and signed the form were recruited in the study. The participants were briefed on MR safety and the potential risks of the examination. The safety screening was carried out and recorded on the MR safety checklist.

Study Setting and Scanning Protocol

The research was conducted using an Ingenia 3.0 T MRI scanner (Philips Healthcare) at the Radiology Department, Hospital Pengajar UPM, Universiti Putra Malaysia, Serdang. Throughout the scanning, the participant remained supine and in a head-first position. The eight-channel receivers (Rx) dedicated shoulder coil (DSC) fitted securely over the affected

shoulder, and the laser beam was centred over the coil. The participant was secured with straps and padded with designated sponges. The participant was scanned using the standard, non-contrast shoulder protocol (axial proton density fat saturation; PDFS, coronal oblique T1, coronal oblique T2, coronal oblique PDFS, sagittal oblique PDFS, and sagittal oblique T2 fat saturation; FS) with the addition of the coronal oblique PROPELLER proton density fat saturation (PROPELLER PDFS) pulse sequence as tabulated in Table II. The entire sequences were repeated then, using a small flex coil (SFC) for image quality comparison.

Data Collection

Two certified radiologists with more than three years of experience in magnetic resonance imaging (MRI) and ultrasound (US) musculoskeletal (MSK) imaging, independently evaluated and graded image artifact reduction between standard coronal oblique PDFS and coronal oblique PROPELLER PDFS images using a five-point scale (0: no visualisation and 4: severe visualisation). The SNR and CNR were then quantitatively evaluated between sequences and with various RF coils (DSC and SFC). Three 2cm-elliptical-ROIs were measured at the humerus bone (SNR_A), glenohumeral joint (SNR_B), and supraspinatus tendon (SNR_C) for SNR measurements. For the CNR, nine 2cm elliptical ROIs were measured between fat-fluid (FT-FL), fat-tendon (FT-TDN), fat-bone (FT-BN), fat-muscle (FT-MS), bone-fluid (BN-FL), bone-tendon (BN-TDN), bone-muscle (BN-MS), muscle-fluid (MS-FL), and muscle-tendon (MS-TDN).

Statistical Analysis

The data were analyzed with IBM Statistical Package for Social Science (SPSS) version 26.0 software. The Shapiro-Wilk test was done to assess the normality of the data, and the findings indicate a non-normal distribution. A non-parametric Wilcoxon Signed Ranks test was performed to examine the reduction of image artifact between standard coronal oblique PDFS and coronal oblique PROPELLER PDFS pulse sequences using different types of RF coils. The agreement between the two observers was measured using kappa statistics. The SNR and CNR values between pulse sequences were quantitatively analyzed using the Mann-Whitney U test.

Ethics Approval And Informed Consent

The participation of each participant in this research was entirely voluntary. Prior to scanning, the subject information sheet, consent form, MR safety, and possible risk and injury were explained and documented. The study was approved by the Universiti Teknologi MARA (UiTM) research ethics committee (FERC/FSK/MR/2022/0281) and Ethics Committee for Research Involving Human Subject (JKEUPM), Universiti Putra Malaysia (JKEUPM-2022-928) and adhered to the Declaration of Helsinki 1964.

RESULTS

Image Artifact Reduction between Standard Coronal Oblique PDFS and Coronal Oblique PROPELLER PDFS

Comparing motion and pulsation artifact reduction using SFC, the coronal oblique PROPELLER PDFS pulse sequence significantly reduced both motion and pulsation artifact

Table I: Inclusion and exclusion criteria

Inclusion criteria:	
1.	Participants age between 18-85years old.
2.	Male and non-pregnant female.
3.	No contraindication to MRI.
4.	Clinical diagnosis of traumatic shoulder injuries (i.e tendon and ligament injury, impingement, rotator cuff tear etc).
5.	Informed consent from participants.
Exclusion criteria:	
1.	Participants with body weight above 95 kilogrammes.
2.	Claustrophobia and MRI incompatible.
3.	Participants who are pregnant.
4.	Clinical diagnosis of shoulder tumour, infectious disease and metabolic changes.

Table II: MRI Shoulder protocol

Sequence	TR (ms)	TE (ms) method	Slice thickness (mm)	FOV (mm)	K-space filling
Axial PDFS	2552	30	3.0	150	Cartesian
Sagittal oblique PDFS	2500	30	3.0	160	
Sagittal oblique T2 FS	3593	87	3.0	160	
Coronal oblique T1	595	18	3.0	160	
Coronal oblique T2	3000	87	3.0	160	
Coronal oblique PDFS	2500	30	3.0	160	
Additional sequence					
Coronal oblique PROPELLER PDFS	2500	30	3.0	160	PROPELLER

Table III: Mean score image artifact reduction comparison between standard PDFS and PROPELLER PDFS sequences using SFC

Type of artifact, Observer	Small Flex Coil (SFC)			
	Standard PDFS	PROPELLER PDFS	Z-score	p-value
	Mean ± SD (Md)	Mean ± SD (Md)		
Motion artifact (n=18)				
Observer 1	1.83 ± 1.04 (2.0)	0.83 ± 0.71 (1.0)	-3.286	0.001*
Observer 2	1.67 ± 0.91 (2.0)	0.89 ± 0.58 (1.0)	-3.071	0.002*
Kappa, κ	0.541	0.850		
Pulsation artifact (n=18)				
Observer 1	1.17 ± 0.62 (1.0)	0.67 ± 0.69 (1.0)	-3.00	0.003*
Observer 2	1.22 ± 0.55 (1.0)	0.61 ± 0.70 (0.5)	-3.317	0.001*
Kappa, κ	0.390	0.866		

Notes: Results above are rating by observers formatted as Mean ± Standard Deviation and Medan in parenthesis. Except for Kappa value, Z-score and p-value were calculated using Wilcoxon Signed Rank Test.
 * p-value is significant at <0.05 level.
 ** p-value is significant at <0.001 level.

Table IV: Mean score image artifact reduction comparison between standard PDFS and PROPELLER PDFS sequences using DSC

Type of artifact, Observer	Dedicated Shoulder Coil (DSC)			
	Standard PDFS	PROPELLER PDFS	Z-score	p-value
	Mean ± SD (Md)	Mean ± SD (Md)		
Motion artifact (n=18)				
Observer 1	2.06 ± 1.00 (2.0)	1.11 ± 0.83 (1.0)	-3.494	<0.001**
Observer 2	1.83 ± 0.92 (2.0)	1.06 ± 0.64 (1.0)	-3.276	0.001*
Kappa, κ	0.741	0.224		
Pulsation artifact (n=18)				
Observer 1	1.17 ± 0.51 (1.0)	0.56 ± 0.51 (1.0)	-3.317	0.001*
Observer 2	1.22 ± 0.43 (1.0)	0.50 ± 0.51 (0.5)	-3.606	<0.001**
Kappa, κ	0.286	0.543		

Notes: Results above are rating by observers formatted as Mean ± Standard Deviation and Medan in parenthesis. Except for Kappa value, Z-score and p-value were calculated using Wilcoxon Signed Rank Test.
 * p-value is significant at <0.05 level.
 ** p-value is significant at <0.001 level.

Table V: Signal-to-noise ratio (SNR) of standard PDFS and PROPELLER PDFS sequences using SFC and DSC

Image Quality	Small Flex Coil (SFC)			
	Standard PDFS	PROPELLER PDFS	Z-score	p-value
	Mean Rank	Mean Rank		
SNR				
SNR _A	22.22	14.78	-2.120	.034*
SNR _B	25.83	11.17	-4.176	<.001**
SNR _C	25.44	11.56	-3.955	<.001**
	Dedicated Shoulder Coil (DSC)			
	Mean Rank	Mean Rank	Z-score	p-value
SNR				
SNR _A	24.50	12.50	-3.417	<.001**
SNR _B	26.72	10.28	-4.683	<.001**
SNR _C	25.83	11.17	-4.176	<.001**

Note: Results above are values from Region of Interest (ROI) formatted as Mean Rank generated from Mann-Whitney U Test. Z-score and p-value were also calculated using Mann-Whitney U Test.

* p-value is significant at <0.05 level.

** p-value is significant at <0.001 level.

SNR_A = humerus bone, SNR_B = glenohumeral joint, SNR_C = supraspinatus tendon.

Table VI: Contrast-to-noise ratio (CNR) of standard PDFS and PROPELLER PDFS sequences using small SFC

Image Quality	Small Flex Coil (SFC)			
	Standard PDFS	PROPELLER PDFS	Z-score	p-value
	Mean Rank	Mean Rank		
CNR				
CNR _{FT-FL}	13.67	23.33	-2.753	0.006*
CNR _{FT-TDN}	17.22	19.78	-0.728	0.467
CNR _{FT-BN}	25.33	11.67	-3.892	<0.001**
CNR _{FT-MS}	19.94	17.06	-0.823	0.411
CNR _{BN-FL}	11.06	25.94	-4.240	<0.001**
CNR _{BN-TDN}	10.94	26.06	-4.303	<0.001**
CNR _{BN-MS}	11.06	25.94	-4.240	<0.001**
CNR _{MS-FL}	12.94	24.06	-3.164	0.002*
CNR _{MS-TDN}	15.17	21.83	-1.898	0.0580

Note: Results above are values from Region of Interest (ROI) formatted as Mean Rank generated from Mann-Whitney U Test. Z-score and p-value were also calculated using Mann-Whitney U Test.

* p-value is significant at <0.05 level.

** p-value is significant at <0.001 level.

CNR_{FT-FL} = between fat-fluid, CNR_{FT-TDN} = between fat-tendon, CNR_{FT-BN} = between fat-bone, CNR_{FT-MS} = between fat-muscle, CNR_{BN-FL} = between bone-fluid, CNR_{BN-TDN} = between bone-tendon, CNR_{BN-MS} = between bone-muscle, CNR_{MS-FL} = between muscle-fluid and CNR_{MS-TDN} = between muscle-tendon.

Table VII: Contrast-to-noise ratio (CNR) of standard PDFS and PROPELLER PDFS sequences using DSC

Image Quality	Dedicated Shoulder Coil (DSC)			
	Standard PDFS	PROPELLER PDFS	Z-score	p-value
	Mean Rank	Mean Rank		
CNR				
CNR _{FT-FL}	11.39	25.61	-4.050	<0.001**
CNR _{FT-TDN}	13.50	23.50	-2.847	0.004*
CNR _{FT-BN}	26.39	10.61	-4.493	<0.001**
CNR _{FT-MS}	23.50	13.50	-2.848	0.004*
CNR _{BN-FL}	10.06	26.94	-4.809	<0.001**
CNR _{BN-TDN}	10.94	26.06	-4.303	<0.001**
CNR _{BN-MS}	9.94	27.06	-4.872	<0.001**
CNR _{MS-FL}	10.72	26.28	-4.429	<0.001**
CNR _{MS-TDN}	14.22	22.78	-2.436	0.014*

Note: Results above are values from Region of Interest (ROI) formatted as Mean Rank generated from Mann-Whitney U Test. Z-score and p-value were also calculated using Mann-Whitney U Test.

* p-value is significant at <0.05 level.

** p-value is significant at <0.001 level.

CNR_{FT-FL} = between fat-fluid, CNR_{FT-TDN} = between fat-tendon, CNR_{FT-BN} = between fat-bone, CNR_{FT-MS} = between fat-muscle, CNR_{BN-FL} = between bone-fluid, CNR_{BN-TDN} = between bone-tendon, CNR_{BN-MS} = between bone-muscle, CNR_{MS-FL} = between muscle-fluid and CNR_{MS-TDN} = between muscle-tendon.

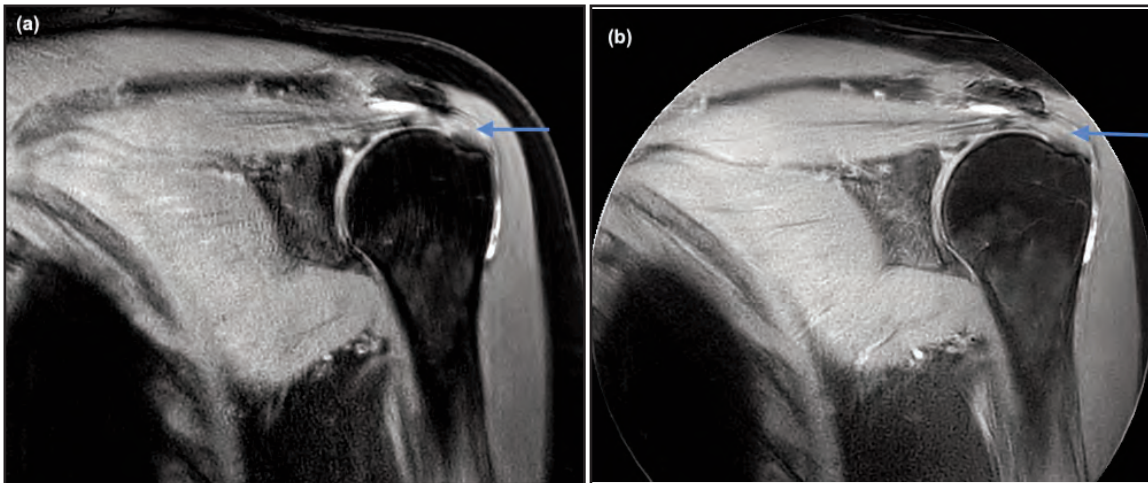


Fig. 1: Shoulder MR images as standard coronal oblique with motion artifact (a: blue arrow) and coronal oblique PROPELLER PDFS with reduction of motion artifact (b: blue arrow)

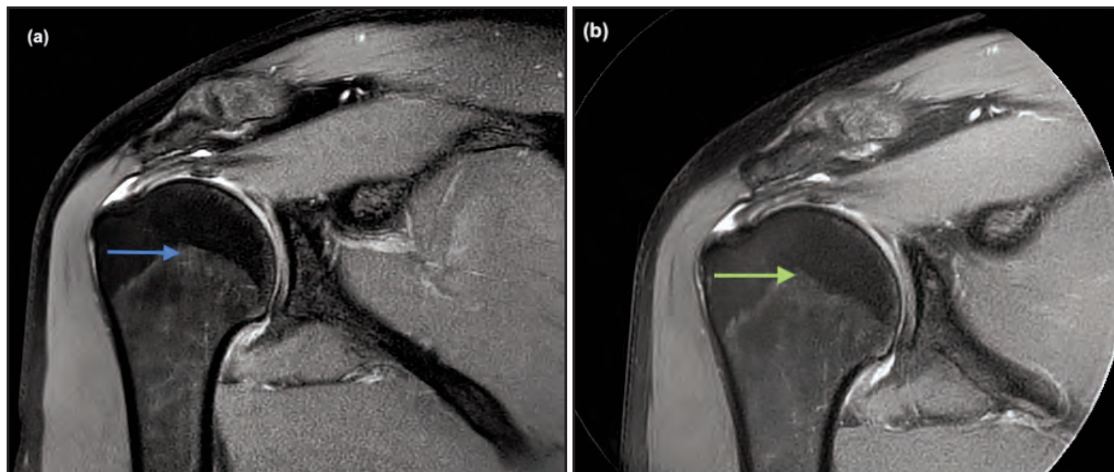


Fig. 2: (a) Shoulder image of a standard coronal oblique with PDFS image revealing the presence of motion artefact at the humeral bone (blue arrow). In contrast, (b) displays a coronal oblique PROPELLER PDFS image, which exhibits an artifact-free image with a clear depiction of the humeral bone (green arrow) and the supraspinatus tendon. Both images were acquired using a small flex coil (SFC)

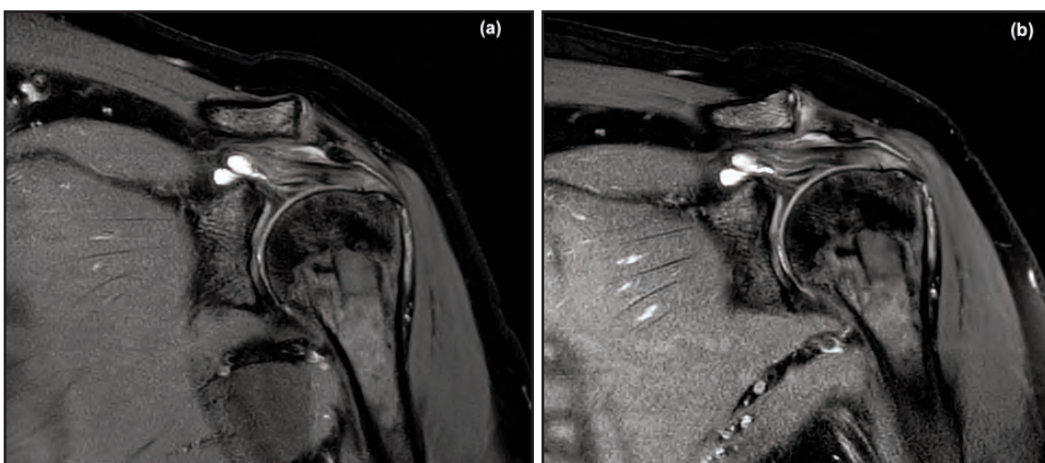


Fig. 3: (a) Standard coronal oblique PDFS image revealed cartilage with a tendon-like appearance. (b) Coronal oblique PROPELLER PDFS show a distinct contrast between cartilage and the surrounding bone, muscle, and soft tissue. Both images were acquired using a dedicated shoulder coil (DSC)

compared to standard coronal oblique PDFS pulse sequence ($p < 0.05$) (Fig. 1-3 and Table III). Furthermore, the coronal oblique PROPELLER PDFS pulse sequence also significantly reduced both motion and pulsation artifacts when compared to standard coronal oblique PDFS ($p < 0.05$) when scanned with DSC (Table IV).

Signal-to-noise Ratio (SNR) between Standard Coronal Oblique PDFS and Coronal Oblique PROPELLER PDFS by Using Various RF Coils

Signal-to-noise ratio (SNR) was measured from the humerus bone (SNR_A), glenohumeral joint (SNR_B), and supraspinatus tendon (SNR_C) using both sequences and coil types. The mean rank of the SNR of the standard coronal oblique PDFS pulse sequence was statistically significant compared to the coronal oblique PROPELLER PDFS pulse sequence when using both coil types ($p = 0.034$ and $p < 0.001$) (Table V).

Contrast-to-noise Ratio (CNR) between Standard Coronal Oblique PDFS and Coronal Oblique PROPELLER PDFS by Using Various RF Coils

Contrast-to-noise ratio (CNR) between standard coronal oblique PDFS pulse sequence and coronal oblique PROPELLER PDFS pulse sequence were measured from nine points; between fat-fluid (CNR_{FT-FL}), between fat-tendon (CNR_{FT-TDN}), between fat-bone (CNR_{FT-BN}), between fat-muscle (CNR_{FT-MS}), between bone-fluid (CNR_{BN-FL}), between bone-tendon (CNR_{BN-TDN}), between bone-muscle (CNR_{BN-MS}), between muscle-fluid (CNR_{MS-FL}) and between muscle-tendon (CNR_{MS-TDN}). The CNR of coronal oblique PROPELLER PDFS pulse sequence using SFC were statistically significant between fat-fluid ($p = 0.006$), between bone-fluid, between bone-tendon, between bone-muscle ($p < 0.001$, respectively) and between muscle-fluid ($p = 0.002$). However, the CNR between fat-bone and fat-muscle was significantly higher in the standard PDFS pulse sequence (Table VI).

The CNR of the coronal oblique PROPELLER PDFS pulse sequence was statistically significant and had a higher mean rank than the standard coronal oblique PDFS pulse sequence when using DSC. Significant and higher mean ranks were found between fat-fluid ($p < 0.001$), between fat-tendon ($p = 0.004$), between bone-fluid, between bone-tendon, between bone-muscle, between muscle-fluid ($p < 0.001$, respectively), and between muscle-tendon ($p = 0.014$). Similar to the CNR measurement obtained from SFC, the CNR between fat-bone and fat-muscle was significantly higher when the standard PDFS pulse sequence was used with DSC (Table VII).

Inter-rater Reliability Kappa Test (IRR Kappa Test)

IRR Kappa test was run to determine if there was an agreement between two musculoskeletal (MSK) radiologists on image artifact reduction when scanned with standard PDFS and PROPELLER PDFS pulse sequences by using a small flex coil (SFC) and dedicated shoulder coil (DSC). There was moderate and fair agreement between radiologists in evaluating motion and pulsation artifact reduction from standard PDFS pulse sequence using small flex coil (SFC) with $\kappa = 0.541$ and $\kappa = 0.390$ respectively. While for the PROPELLER PDFS pulse sequence, there was perfect agreement between radiologists in evaluating motion artifact reduction with

$\kappa = 0.850$ and pulsation artifact reduction with $\kappa = 0.866$ (Table III).

When scanned with standard PDFS pulse sequence using a dedicated shoulder coil (DSC), the inter-rater reliability for the raters was found to be a substantial and fair agreement in evaluating motion and pulsation artifact reduction with $\kappa = 0.741$ and $\kappa = 0.286$ respectively, and fair and moderate agreement of motion artifact reductions with $\kappa = 0.224$ and pulsation artifact reduction with $\kappa = 0.543$ when scanned with PROPELLER PDFS pulse sequence using DSC (Table IV).

DISCUSSION

PROPELLER significantly reduces motion and pulsation artifacts. These findings are consistent with those of studies by Dietrich et al.,¹⁵ Lavdas et al.,¹¹ and Nagatomo et al.¹⁶ PROPELLER is a robust motion correction technique that acquires k-space with multiple echo train length (ETL) that is rotated around the center of k-space like rotating bars or blades of readout that focuses on the region with the highest contrast and signal amplitude, the center of k-space.^{19,20} Repetitive sampling and oversampling of the higher contrast/signal center of k-space compensate for translational and rotational motion artifacts by eliminating inconsistent data resulting from motion during the scan.^{19,21} Artifact reduction was also accomplished by increasing the receiver bandwidth (rBw) and ETL parameters¹¹ in addition to the blade width and k-space coverage.²² PROPELLER acquisition has been shown to significantly reduce or eliminate motion artifacts in a variety of clinical applications, including the shoulder,^{15,16} bladder,²³ spine,²¹ knee²⁴ and pulsatile flow artifacts in the brain and neck.²¹ Propellers have been successfully applied to MRIs of the brain in uncooperative or paediatric patients and are also recommended for free breathing unsedated MRI in children.^{19,25}

The quantitative analysis of the SNR sequences with different RF coils revealed that the standard coronal oblique PDFS were significantly superior to the coronal oblique PROPELLER PDFS. The repetitive, oversampling, and multishot nature of PROPELLER k-space filling enhances image quality, but not SNR. The SNR decreases when blades are combined to occupy the k-space because of the unequal distribution of data.²⁶ However, the SNR can be enhanced by acquiring data for a longer scanning time.^{23,27} In PROPELLER, the number of blades acquired to traverse the entire k-space is approximately $N = \pi/2 \times M/ETL$ ($M = \text{matrix size}$); this is approximately a factor of $\pi/2$ longer than standard sequence.²⁷ In this study, the system-predetermined PROPELLER scanning duration was ten seconds longer than the standard sequence, which was insufficient to achieve a higher SNR than the standard sequence. Meanwhile, the quantitative analysis of the CNR revealed that PROPELLER was significantly superior to the standard sequence, consistent with the study by Forbes et al., CNR is enhanced because of the uniform distribution of echo time across the k-space.²⁶

Higher CNR between fat-bone and fat-muscle in standard coronal oblique PDFS pulse sequence was consistent with findings

from previous studies.^{11,20,28} CNR is a difference between the SNR or signal intensity (SI) of adjacent regions or tissues. The image contrast primarily depends on intrinsic and extrinsic factors. The elements that influence SNR also control CNR. The increased CNR seen between the tissues in this study may be attributed to the SNR and distinctive tissue properties in conjunction with the use of the PROPELLER technique.^{28,29} Furthermore, the noise distribution across the entire coil can be influenced by the type of coil, particularly when employing a new coil system and reconstruction techniques. This, in turn, can have an impact on the measurements of SNR and CNR.³⁰

The inter-rater agreement for image artifact reduction on coronal oblique PROPELLER PDFS was found to be perfect when scanned using the SFC, whereas it was seen to be fair to moderate when scanned using the DSC. The image quality improved while utilising SFC due to the secure fitting of the coil to the region of interest, irrespective of the patient's body habitus. Moreover, the coronal oblique PROPELLER PDFS demonstrated superior inter-rater agreement in comparison to the standard coronal oblique PDFS. The findings suggest that the application of PROPELLER PDFS could potentially be beneficial in eliminating motion artefacts in clinical shoulder MRI.

Our study had some limitations. One limitation of this study was the limited size of the sample. The small sample size was mainly attributed to the study's inclusion criteria, which specifically focused on participants who had clinical diagnoses for traumatic shoulder injuries. Further research could encompass broader range of shoulder pathologies, such as tumours, infectious diseases, metabolic changes and movement disorder such as Parkinson's disease. A further limitation of this study was the utilisation of a dedicated shoulder coil in a patient with small habitus. The small body habitus caused the shoulder to not fit properly within the coil, resulting in a gap between the shoulder and the coil. The existence of the gap contributes to the degradation of the SNR, thus resulting in a reduction in the image's quality. It is recommended that in future research, appropriate measures should be taken to ensure that the patient's shoulder and body habitus are suitably immobilised within the coil. The absence of repetitive measurements was another limitation of this study. Each observer provided a single score for the image, and no subsequent measurements were conducted. Hence, intra-rater variability, a measure used to evaluate the degree of consistency demonstrated by a single observer across different time intervals, is therefore impossible to achieve

CONCLUSION

The utilization of the PROPELLER technique has the potential to effectively eliminate motion and pulsation artefacts in shoulder MRI when compared to the standard PDFS sequence. The total scanning time for the PROPELLER PDFS sequence in this study was 4 minutes and 35 seconds, ten seconds longer than for standard PDFS (4 minutes and 25 seconds), with this additional ten seconds mainly due to the k-space filling method. Furthermore, both SFC and DSC has been found to enhance the image quality when employing

with coronal oblique PROPELLER technique. This technique has the potential to substitute the standard coronal oblique PDFS sequences of the MRI of the shoulder.

ACKNOWLEDGEMENTS

The authors would like to express our gratitude to the Head of the Radiology Department, Hospital Pengajar Universiti Putra Malaysia for granting permission to use the facility, as well as the volunteer who voluntarily participated in this research.

CONFLICT OF INTEREST

The authors of this study declare that there are no conflicts of interest.

FUNDING

No funding received.

REFERENCES

- King LJ, Healy JC, Baird P. Imaging of the rotator cuff and biceps tendon. *J R Army Med Corps.* 1999;145(3):125-31.
- Everhart JS, Abouljoud MM, Kirven JC, Flanigan DC. Full-thickness cartilage defects are important independent predictive factors for progression to total knee arthroplasty in older adults with minimal to moderate osteoarthritis: data from the osteoarthritis initiative. *JBJS* 2019; 101: 56-63.
- Jungmann PM, Gersing AS, Woertler K, Dietrich TJ, Baum T, Baumann F, et al., Reliable semiquantitative whole-joint MRI score for the shoulder joint: The shoulder osteoarthritis severity (SOAS) score. *Journal of Magnetic Resonance Imaging* 2019;49: e152-63.
- Ashby K, Adams BN, Shetty M. StatPearls [Internet]. Treasure Island (FL): StatPearls Publishing; 2022. Appropriate Magnetic Resonance Imaging Ordering. [cited 23 January 20]. Available from: <https://www.ncbi.nlm.nih.gov/books/NBK565857/>
- Goh CK, Peh WC. Pictorial essay: pitfalls in magnetic resonance imaging of the shoulder. *Can Assoc Radiol J* 2012; 63(4): 247-59.
- Niitsu M, Saruya S, Sakaguchi K, Watarai K, Yoneyama M, Katsumata Y, et al., Motion-robust MR imaging of the shoulder using compressed SENSE MultiVane. *European Journal of Radiology Open.* 2022; 9: 100450.
- Solomon O, Patriat R, Braun H, Palnitkar TE, Moeller S, Auerbach EJ, et al., Motion robust magnetic resonance imaging via efficient Fourier aggregation. *Medical Image Analysis.* 2023; 83: 102638.
- Stucht D, Danishad KA, Schulze P, Godenschweger F, Zaitsev M, Speck O. Highest resolution in vivo human brain MRI using prospective motion correction. *PLoS one.* 2015; 10(7): e0133921.
- White N, Roddey C, Shankaranarayanan A, Han E, Rettmann D, Santos J, et al., PROMO: real-time prospective motion correction in MRI using image-based tracking. *Magnetic Resonance in Medicine: An Official Journal of the International Society for Magnetic Resonance in Medicine.* 2010; 63(1): 91-105.
- Haacke EM, Lenz GW. Improving MR image quality in the presence of motion by using rephasing gradients. *American journal of roentgenology.* 1987; 148(6): 1251-8.
- Lavdas E, Vlychou M, Zaloni E, Vassiou K, Tsagkalis A, Dailiana Z, et al. Elimination of motion and pulsation artifacts using BLADE sequences in shoulder MR imaging. *Skeletal Radiol* 2015; 44(11): 1619-26.
- Dean Deyle G. The role of MRI in musculoskeletal practice: a clinical perspective. *J Man Manip Ther* 2011; 19(3): 152-61.

13. Shimamoto H, Tsujimoto T, Kakimoto N, Majima M, Iwamoto Y, Senda Y, et al. Effectiveness of the periodically rotated overlapping parallel lines with enhanced reconstruction (PROPELLER) technique for reducing motion artifacts caused by mandibular movements on fat-suppressed T2-weighted magnetic resonance (MR) images. *Magn Reson Imaging* 2018; 54: 1-7.
14. Chen X, Xian J, Wang X, Wang Y, Zhang Z, Guo J, et al. Role of periodically rotated overlapping parallel lines with enhanced reconstruction diffusion-weighted imaging in correcting distortion and evaluating head and neck masses using 3 T MRI. *Clin Radiol* 2014; 69(4): 403-9.
15. Dietrich TJ, Ulbrich EJ, Zanetti M, Fucentese SF, Pfirrmann CW. PROPELLER technique to improve image quality of MRI of the shoulder. *AJR Am J Roentgenol* 2011; 197(6): W1093-100.
16. Nagatomo K, Yabuuchi H, Yamasaki Y, Narita H, Kumazawa S, Kojima T, et al., Efficacy of periodically rotated overlapping parallel lines with enhanced reconstruction (PROPELLER) for shoulder magnetic resonance (MR) imaging. *Eur J Radiol*. 2016; 85(10): 1735-43.
17. Mulyati S, Rusyadi L, Rahmawati IM, Wibowo AS, Indrati R. Differentiation image quality of MRI shoulder joint with variation RF coils. *E3S Web of Conferences* 2019; 125: 180.
18. Kathiravan S, Kanakaraj J. A review on potential issues and challenges in MR imaging. *ScientificWorldJournal* 2013; 2013: 783-15.
19. Janos S, Schooler GR, Ngo JS, Davis JT. Free-breathing unsedated MRI in children: Justification and techniques. *J Magn Reson Imaging* 2019; 50(2): 365-76.
20. Fellner C, Menzel C, Fellner FA, Ginthoer C, Zorger N, Schreyer A, et al. BLADE in sagittal T2-weighted MR imaging of the cervical spine. *AJNR Am J Neuroradiol* 2010; 31(4): 674-81.
21. Ragoschke-Schumm A, Schmidt P, Schumm J, Reimann G, Mentzel HJ, Kaiser WA, et al. Decreased CSF-flow artefacts in T2 imaging of the cervical spine with periodically rotated overlapping parallel lines with enhanced reconstruction (PROPELLER/BLADE). *Neuroradiology* 2011; 53(1): 13-8.
22. Hirokawa Y, Isoda H, Maetani YS, Arizono S, Shimada K, Togashi K. Evaluation of motion correction effect and image quality with the periodically rotated overlapping parallel lines with enhanced reconstruction (PROPELLER) (BLADE) and parallel imaging acquisition technique in the upper abdomen. *J Magn Reson Imaging* 2008; 28(4): 957-62.
23. Nguyen HT, Shah ZK, Mortazavi A, Pohar KS, Wei L, Zynger DL, et al. Periodically rotated overlapping parallel lines with enhanced reconstruction acquisition to improve motion-induced artifacts in bladder cancer imaging: Initial findings. *Medicine (Baltimore)*. 2019; 98(42): e17075.
24. Lavdas E, Mavroidis P, Hatzigeorgiou V, Roka V, Arikidis N, Oikonomou G, et al. Elimination of motion and pulsation artifacts using BLADE sequences in knee MR imaging. *Magn Reson Imaging* 2012; 30(8): 1099-110.
25. Michaely HJ, Kramer H, Weckbach S, Dietrich O, Reiser MF, Schoenberg SO. Renal T2-weighted turbo-spin-echo imaging with BLADE at 3.0 Tesla: initial experience. *J Magn Reson Imaging* 2008; 27(1): 148-53.
26. Forbes KP, Pipe JG, Bird CR, Heiserman JE. PROPELLER MRI: clinical testing of a novel technique for quantification and compensation of head motion. *J Magn Reson Imaging* 2001; 14(3): 215-22.
27. Wintersperger BJ, Runge VM, Biswas J, Nelson CB, Stemmer A, Simonetta AB, et al. Brain magnetic resonance imaging at 3 Tesla using BLADE compared with standard rectilinear data sampling. *Invest Radiol* 2006; 41(7): 586-92.
28. Yoneyama M, Nakamura M, Obara M, Okuaki T, Sashi R, Sawano S, et al. Hyperecho PROPELLER-MRI: Application to rapid high-resolution motion-insensitive T2-weighted black-blood imaging of the carotid arterial vessel wall and plaque. *J. Magn. Reson. Imaging*, 2017; 45: 515-24.
29. Jiang H, Wang S, Xian J, Chen Q, Wei W. Efficacy of PROPELLER in reducing ocular motion artefacts and improving image quality of orbital MRI at 3 T using an eye surface coil. *Clinical Radiology*. 2019; 74(9): 734-e7.
30. Dietrich O, Raya JG, Reeder SB, Reiser MF, Schoenberg SO. Measurement of signal-to-noise ratios in MR images: Influence of multichannel coils, parallel imaging, and reconstruction filters. *J. Magn. Reson. Imaging*, 2007; 26: 375-85.